FEBS Letters 588 (2014) 2301–2306

journal homepage: www.FEBSLetters.org

Resonance Raman and FTIR spectroscopic characterization of the closed and open states of channelrhodopsin-1

Vera Muders [a], Silke Kerruth [b], Víctor A. Lórenz-Fonfría [b], Christian Bamann [c], Joachim Heberle [b], Ramona Schlesinger [a,*]

[a] Genetic Biophysics, Freie Universität Berlin, 14195 Berlin, Germany
[b] Experimental Molecular Biophysics, Freie Universität Berlin, 14195 Berlin, Germany
[c] Max-Planck-Institute of Biophysics, Department of Biophysical Chemistry, 60438 Frankfurt/Main, Germany

ARTICLE INFO

Article history:
Received 28 April 2014
Revised 9 May 2014
Accepted 9 May 2014
Available online 21 May 2014

Edited by Peter Brzezinski

Keywords:
Channelrhodopsin
*Ca*ChR1
Optogenetics
Retinal
Photoreceptor
Resonance Raman spectroscopy

ABSTRACT

Channelrhodopsin-1 from *Chlamydomonas augustae* (*Ca*ChR1) is a light-activated cation channel, which is a promising optogenetic tool. We show by resonance Raman spectroscopy and retinal extraction followed by high pressure liquid chromatography (HPLC) that the isomeric ratio of all-*trans* to 13-*cis* of solubilized channelrhodopsin-1 is with 70:30 identical to channelrhodopsin-2 from *Chlamydomonas reinhardtii* (*Cr*ChR2). Critical frequency shifts in the retinal vibrations are identified in the Raman spectrum upon transition to the open (conductive P_2^{380}) state. Fourier transform infrared spectroscopy (FTIR) spectra indicate different structures of the open states in the two channelrhodopsins as reflected by the amide I bands and the protonation pattern of acidic amino acids.

© 2014 The Authors. Published by Elsevier B.V. on behalf of the Federation of European Biochemical Societies. This is an open access article under the CC BY-NC-ND license (http://creativecommons.org/licenses/by-nc-nd/3.0/).

1. Introduction

Channelrhodopsins (ChRs) are photoreceptors originally located in the eyespot of unicellular green algae initiating phototactic and photophobic responses in order to swim towards perfect light conditions [1]. When heterologously expressed in animal cells, ChRs act as light-gated cation channels and hence are used as optogenetic tools to depolarize nerve cells by light. Optogenetics is a promising field to study neurophysiological diseases and to potentially restore vision to blind patients.

Much effort has been invested in improving ChRs for optogenetic applications, either by tuning existing ChRs [2] or by screening novel ones [3]. Desirable features of ChRs are a unitary high conductance, slow inactivation upon sustained illumination and a red-shifted absorption maximum. The first two would allow achieving light-driven membrane depolarization at lower expression levels and the latter to minimize light scattering of biological tissue allowing for deeper penetration depth of the excitation light. Earlier studies have reported that channelrhodopsin-1 from *Chlamydomonas augustae* (*Ca*ChR1) exhibits a slower inactivation of the generated photocurrents compared to channelrhodopsin-1 from *Chlamydomonas reinhardtii* (*Cr*ChR1) [3]. In addition *Ca*ChR1 shows an absorption maximum of 520 nm, which is red-shifted compared to 470 nm of the widely used channelrhodopsin-2 from *Chlamydomonas reinhardtii* (*Cr*ChR2). The lack of fast inactivation and the red-shifted absorption maximum render *Ca*ChR1 a promising tool for optogenetic applications. However, the functional expression of *Ca*ChR1 in mammalian cells requires optimization due to the low binding affinity to retinal [3].

Despite the fact that channelrhodopsins are widely used in optogenetic applications, our knowledge on the molecular mechanism is far from satisfactory [4]. The crystal structure of a chimera construct of *Cr*ChR1 (helices A–E) and *Cr*ChR2 (helices F and G) displays a dimer where each monomer comprises a

Abbreviations: *Ca*ChR1, channelrhodopsin-1 from *Chlamydomonas augustae*; *Cr*ChR2, channelrhodopsin-2 from *Chlamydomonas reinhardtii*; HPLC, high pressure liquid chromatography; FTIR, Fourier transform infrared spectroscopy; RR, resonance Raman; RSB, retinal Schiff base; DDM, *n*-dodecyl-β-D-maltopyranoside; BR, bacteriorhodopsin; *Hs*SRII, sensory rhodopsin II from *Halobacterium salinarum*; *Np*SRII, sensory rhodopsin II from *Natronomonas pharaonis*; FWHM, full width at half maximum

* Corresponding author. Address: Freie Universität Berlin, Genetic Biophysics, Arnimallee 14, 14195 Berlin, Germany. Fax: +49 30 838 56510.
E-mail address: r.schlesinger@fu-berlin.de (R. Schlesinger).

http://dx.doi.org/10.1016/j.febslet.2014.05.019
0014-5793/© 2014 The Authors. Published by Elsevier B.V. on behalf of the Federation of European Biochemical Societies.
This is an open access article under the CC BY-NC-ND license (http://creativecommons.org/licenses/by-nc-nd/3.0/).

hydrophilic pore surrounded by helices A–C and G. In the closed state, the pore intrudes from the extracellular medium to the middle of the channel, next to the region where the retinal chromophore is bound via a Schiff base to the protein [5]. Fig. 1 shows the retinal covalently bound to K303 of *Ca*ChR1. Spectroscopic studies on *Cr*ChR2 showed that after light excitation the predominant all-*trans* retinal isomerizes to 13-*cis* retinal [6] and the retinal Schiff base (RSB) releases the proton to the primary proton acceptor (D253) [7]. Reprotonation of the RSB from the proton donor (D156) occurs simultaneously with channel closure during the decay of the conductive P_3^{520} intermediate [7]. Electron paramagnetic resonance experiments on *Cr*ChR2 have shown that helices B and F move outwards upon formation of the conductive P_3^{520} state [8]. Such helical movements persist even until the late desensitized P_4^{480} state is formed [9].

Most spectroscopic studies have been performed on *Cr*ChR2, but little is known about the retinal structure and the molecular changes emerging in channelrhodopsin-1 despite the fact that 5 out of 7 helices in the crystallographic structure of the C1C2 chimera were derived from *Cr*ChR1. Time-resolved UV/Vis experiments on solubilized *Ca*ChR1 have identified several photocycle intermediates [10]. Upon illumination, an early P_1^{580} intermediate arises followed by a long-lasting biphasic P_2^{380} intermediate and small contributions of an O-like intermediate at 590 nm [10]. A red-shifted intermediate comparable to the conductive P_3^{520} intermediate of *Cr*ChR2, was not detected. The lifetime of the P_2^{380} state of *Ca*ChR1 correlates with the lifetime of its passive channel current and lies in the ms range. Consequently the P_2^{380} intermediate represents the conductive state of *Ca*ChR1.

In all microbial rhodopsins, the first step in signal transduction after a light pulse comprises the isomerization of the chromophore retinal. Thus, knowledge of the retinal structure in the ground state is mandatory. In this study we determined the retinal isomer composition in the dark state of *Ca*ChR1 by retinal extraction and HPLC analysis. Additionally resonance Raman (RR) and Fourier transform infrared spectroscopy (FTIR) difference spectroscopy in H_2O and D_2O provide information of the retinal structure and the protonation state of the RSB in the dark state as well as in the P_2^{380} intermediate. Furthermore FTIR difference spectra reveal vibrational bands characteristic for protonation changes of carboxylic groups in the open state.

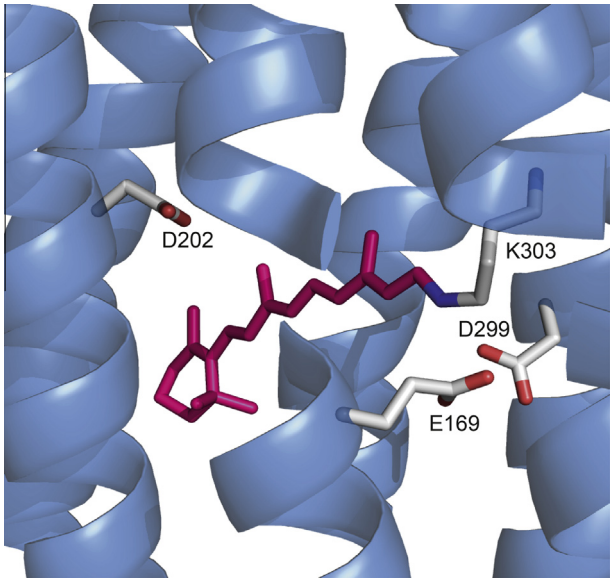

Fig. 1. Retinal binding pocket of *Ca*ChR1. All-*trans* retinal (magenta) is bound via a Schiff base linkage to K303 on helix G. Shown are three carboxylic residues which are possible proton acceptor (E169, D299) and donor groups (D202) of the Schiff base, equivalent to *Cr*ChR2. The structure of *Ca*ChR1 was derived by homology modeling with the SWISS-MODEL server using the C1C2 structure (pdb: 3UG9 [5]) [35–37] as template.

2. Materials and methods

2.1. Cloning, expression and purification of CaChR1

A truncated *Ca*ChR1 gene (1–352 aa; codon optimized for *Pichia pastoris* by GeneArt, Life Technologies) with a 10xHis-tag was inserted into the *Eco*RI and *Not*I restriction sites of the pPIC9K vector (Invitrogen, Carlsbad, CA). To allow recombination into the genome of the yeast *P. pastoris* strain SMD1163 (*his4 pep4 prb1*) the construct was linearized with *Sal*I and transformed by electroporation. Clones were selected on histidine-depleted plates and varying geneticin (G418) concentrations (according to Invitrogen, Multi-Copy *Pichia* Expression Kit). Highly resistant colonies were inoculated into buffered glycerol-complex medium for 24 h. Expression of the main culture in buffered methanol-complex media was induced by addition of 0.5% methanol and 10 μM all-*trans* retinal every 24 h. After 48 h the cells were harvested (6000×*g*, 10 min) and disrupted at 2.7 kbar in a Cell Disrupter (Constant Systems, Model TS, 1.1 kW). Membranes were isolated by centrifugation (186 000×*g*, 1.5 h) and solubilized with 2% *n*-dodecyl-β-D-maltopyranoside (DDM) in 100 mM NaCl, 20 mM HEPES, pH 7.4. The protein was purified via the His-tag on a Ni–NTA affinity column (Macherey–Nagel, Germany). The concentration of *Ca*ChR1 was measured at 518 nm with a UV/Vis spectrometer (Shimadzu).

2.2. Determination of the extinction coefficient by hydroxylamine bleaching

The bleaching of retinal proteins was described earlier [11]. Briefly, solubilized *Ca*ChR1 in 10 mM hydroxylamine was illuminated with cold white light for 45 min while stirring and subsequently adjusted to pH 3. UV/Vis absorption spectra of the sample before and after bleaching were recorded between 250 and 700 nm (UV/Vis spectrometer, Shimadzu), confirming 100% of retinal bleaching (Fig. S1). From the known extinction coefficient of retinal oxime at 360 nm (33 600 $M^{-1}cm^{-1}$[11]) we calculated the extinction coefficient of *Ca*ChR1.

2.3. Retinal extraction and separation by high-pressure liquid chromatography (HPLC)

Retinal extraction from *Ca*ChR1 and quantification of the retinal isomeric composition was done essentially as described [12]. 10 μM of *Ca*ChR1 in 100 mM NaCl, 20 mM HEPES, pH 7.4, 0.05% DDM were stored in the dark at 22 °C for 30 h. For light adaptation, 10 μM of *Ca*ChR1 were illuminated for 10 min using a XBO 75 W light source filtered by a broadband-interference filter (Balzer, 40 nm half bandwidth, centered at 500 nm). Within less than 1 s after the light was turned off, the chromophore of *Ca*ChR1 was extracted with ice-cold ethanol and further isolated by hexane. All steps, except light adaptation, were performed under dim red light. The organic phase containing the extracted retinal was dissolved in 9:1 hexane/ethylacetate and was injected into a normal phase HPLC Merck LaChrom L-7200 system with a ProntoSil 120-3-OH column.

2.4. Light-induced FTIR difference spectroscopy

2–5 μL of solubilized *Ca*ChR1 (5–10 mg protein/mL in 5 mM NaCl, 5 mM HEPES, pH 7.4 with 0.05% DDM) was dried on top of

a BaF_2 window. The protein film was rehydrated from the vapor phase from 3 μL of a glycerol/water solution (2/8 w/w) placed nearby the film. The hydrated film was sealed with a second window with the help of a spacer of 1 mm thickness. Either normal water (H_2O) or deuterium oxide (D_2O) was used. Light-induced IR difference spectra were recorded at 2 cm^{-1} resolution with a FTIR spectrometer (Vertex 80v, Bruker) at 25 °C. The samples were kept in dark for 10 s, and subsequently illuminated for 10 s by an LED emitting at 505 nm. Data acquisition was performed in the last 5 s in dark and in the last 5 s in light. The process was automatically repeated to a final of 3000 co-added scans.

2.5. Resonance Raman spectroscopy

RR spectroscopic measurements have taken place on a LABRAM spectrometer (JobinYvon, Bensheim, Germany) essentially as described [6]. Laser excitation was performed using the emission lines at 647 nm and at 413 nm of a Krypton ion laser (Innova 90C, Coherent, Dieburg, Germany), and the scattering was collected via a microscope objective (10×). The 647 nm line was used to measure the dark state of *Ca*ChR1 under pre-resonance conditions with a spectral resolution of about 2 cm^{-1} spaced by 0.5 cm^{-1}. The 413 nm line was used, to resonantly enhance the blue-shifted P_2^{380} intermediate with a resolution of 4 cm^{-1} spaced by 0.8 cm^{-1}. In the latter experiments, the emission from the second harmonic output of a cw Nd:YAG laser emitting at 532 nm was used to excite the sample. To avoid photobleaching, *Ca*ChR1 was measured in a rotating cell (2800 rpm) in aqueous solution (100 mM NaCl, 20 mM HEPES, pH 7.4, 0.05% DDM). As an internal frequency standard Na_2SO_4 (150 mM) was added to the sample solutions, displaying a specific vibrational band at 979 cm^{-1}. The vibrational bands were fitted by sums of Voigtian line profiles (50% Lorentzian, 50% Gaussian from the OPUS software, Bruker).

3. Results & discussion

We have expressed *Ca*ChR1 in the yeast *P. pastoris* and purified the protein by affinity chromatography. The extinction coefficient of the retinal of *Ca*ChR1 was determined to 36000 $M^{-1}cm^{-1}$ by hydroxylamine bleaching (Fig. S1). The protein solubilized in DDM was subjected to retinal extraction and molecular spectroscopy. RR spectroscopy was applied to provide structural and electronic information on the chromophore retinal. Structural changes of the holoprotein induced by illumination were determined by FTIR difference spectroscopy.

3.1. Retinal structure of dark state CaChR1

To detect the retinal isomer composition in the dark- and light-adapted *Ca*ChR1, retinal was extracted from the protein and the different isomeric forms were separated by HPLC. For the dark-adapted sample 71% all-*trans*, 27% 13-*cis* and 1% 9-*cis* were extracted as calculated by the integral of the chromatogram and the specific extinction coefficient (Fig. 2 and Table S1). The light-adapted protein showed a slightly higher amount of 13-*cis* retinal (33%). Overall, the retinal composition of *Ca*ChR1 agrees well with the retinal composition of *Cr*ChR2 [6] in the dark- and light-adapted state. This is similar to most other microbial sensory rhodopsins [13,14] but different to the ion pumps bacteriorhodopsin (BR) and halorhodopsin which can be driven to 100% all-*trans* retinal by light-adaption [15]. However, reconstitution into lipids can influence the retinal composition as was shown for sensory rhodopsin II from *Halobacterium salinarum* (*Hs*SRII) [11]. The thermostable equilibrium of all-*trans* and 13-*cis* retinal in the dark state of *Ca*ChR1 may present starting points of two different photocycles, as it was proposed for *Cr*ChR2 [16,17].

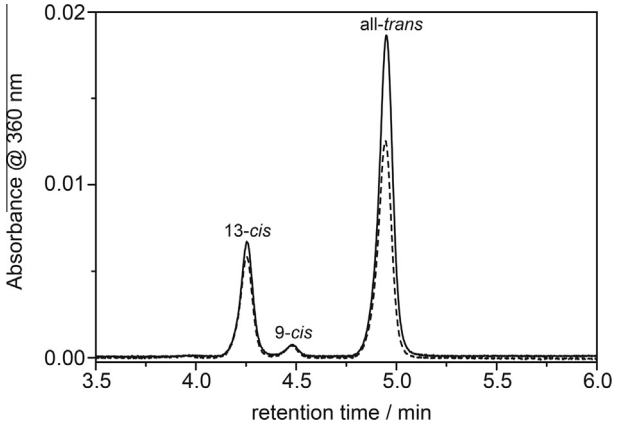

Fig. 2. HPLC of retinal isomers isolated from *Ca*ChR1. The absorption at 360 nm is recorded as a function of the retention time of extracted retinal isomers from dark-adapted *Ca*ChR1 (continuous line) and from light-adapted *Ca*ChR1 (dashed line). The retinal isomers peaked after 4.26 min (13-*cis*), 4.48 min (9-*cis*) and 4.95 min (all-*trans*).

In order to study the retinal configuration in more detail, resonance Raman spectroscopy was applied. Resonance Raman scattering allows enhancement of vibrations selectively from the retinal with marginal contributions from vibrations of the surrounding apoprotein. To measure the dark state of *Ca*ChR1, displaying a λ_{max} = 518 nm, pre-resonant excitation at 647 nm was chosen to minimize light excitation of the protein. The assignment of retinal bands is based on the comparison with resonance Raman spectra of well-studied microbial rhodopsins as BR [15,18–20], *Hs*SRII [21] and *Cr*ChR2 [6,22].

The four C=C double bonds of the retinal couple into four ethylenic modes. Generally, most of the Raman and infrared intensity concentrates in the in-phase mode [19]. This mode appears at 1532 cm^{-1} for the dark state of *Ca*ChR1 (Fig. 3). However, the shape of the band is not symmetric. Band fitting revealed three bands at 1548, 1533 and 1525 cm^{-1} (Fig. S2 and Table S2). Two of these bands were also observed in the FTIR difference spectra at similar wavenumbers, 1550 and 1536 cm^{-1}, respectively (Figs. 5 and S3). For the ethylenic band of *Cr*ChR2, likewise three components were identified. Due to its characteristic blue-shift, the shoulder at 1557 cm^{-1} in *Cr*ChR2, which is analog to the band at 1548 cm^{-1} in *Ca*ChR1, was assigned to the main ethylenic mode of 13-*cis*

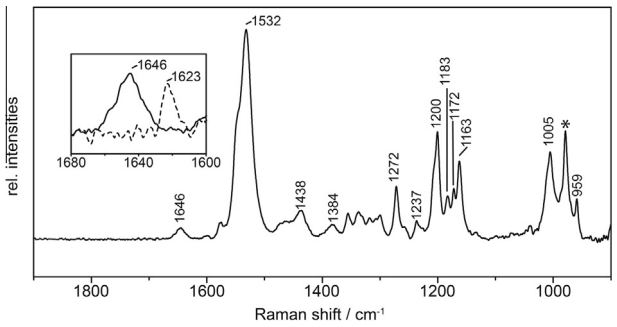

Fig. 3. Raman spectra of *Ca*ChR1. The dark state was probed under pre-resonant conditions using Raman excitation at 647 nm. The inset shows the zoom-out of the frequency region between 1680 and 1600 cm^{-1}. The C=N–H vibrational band of the RSB at 1646 cm^{-1} experienced a downshift of 23 cm^{-1} upon exchange of H_2O (continuous line) to D_2O (dashed line). The band at 979 cm^{-1} (labeled by an asterisk *) is due to the ν_1 vibration of Na_2SO_4 which was added as an internal frequency standard.

retinal [6]. The most intense component at 1533 cm^{-1} (1550 cm^{-1} in *Cr*ChR2) represents the ethylenic vibration of the all-*trans* configuration. The band at 1525 cm^{-1} (1537 cm^{-1} in *Cr*ChR2) might correspond to secondary ethylenic modes from all-*trans* and/or 13-*cis* retinal.

By comparing the integrated area of the bands at 1548 and 1533 cm^{-1} for 13-*cis* and all-*trans*, a relative percentage of 70% all-*trans* and 30% 13-*cis* retinal were calculated for the dark state (Table S2). This is in agreement with the results of the retinal extraction where mainly all-*trans* (71%) and to a minor degree (27%) 13-*cis* retinal were identified (Table S1).

The signal at 1272 cm^{-1} (Fig. 3) is due to in-plane rocking vibrations of vinyl hydrogens [19]. The band at 1005 cm^{-1} corresponds to the in-plane rocking vibration of methyl groups [19]. In the fingerprint region (1250–1100 cm^{-1}), which is indicative for the geometry of the chromophore, the C–C stretching vibrations appear at 1200, 1183, 1172 and 1163 cm^{-1} and are highly mixed combinations of C–C stretches and CCH rocking vibrations. The bands strongly correlate to those observed for *Hs*SRII [21] and indicate the predominance of all-*trans* over 13-*cis* retinal.

The weak band at 1646 cm^{-1} is assigned to the C=N stretching vibration of the RSB [19]. This band undergoes a characteristic downshift to 1623 cm^{-1} upon deuteration (Fig. 3, inset) indicating a protonated RSB. Comparing the frequency to the manifold of well-studied photoreceptors [6], we infer the protonated RSB to be strongly hydrogen bonded. The strong downshift of 23 cm^{-1} upon deuteration and the narrowed bandwidth of the deuterated band from 23 cm^{-1} to 13 cm^{-1} (Fig. 3, inset) was shown to be indicative for the existence of a water molecule in the vicinity of the RSB [6,18,23].

3.2. Retinal structure of the long-lived P_2^{380} photo-intermediate (conductive state)

After light excitation of *Ca*ChR1, a blue-shifted intermediate is formed whose lifetime last until 30 ms and which corresponds to the open (conductive) state of *Ca*ChR1 [10]. Hence, this long-lived intermediate is accumulated under blue–green illumination (λ = 532 nm). Trapping of the open state under photo-stationary conditions is different to *Cr*ChR2, where the closed (desensitized) P_4 state accumulates under continuous illumination [7]. Thus, *Ca*ChR1 provides for the first time the opportunity to characterize the P_2^{380} state of channelrhodopsin by resonance Raman spectroscopy.

The 413 nm emission line of the Kr^+-laser was used to selectively probe the P_2^{380} state (Fig. 4). In comparison to the dark state spectrum, the band of the ethylenic C=C stretching vibration is up-shifted to 1565 cm^{-1}. The frequency up-shift is a consequence of the 13-*cis* configuration of the retinal and the deprotonation of the RSB as was demonstrated on the M states of sensory rhodopsin II from *Natronomonas pharaonis* (*Np*SRII) and BR [24,25]. However, the spectrum still contains minor amounts of all-*trans* retinal, visible by the shoulder at 1532 cm^{-1}.

In the fingerprint region, four bands arise at 1197, 1183, 1174 and 1162 cm^{-1}. The bands at 1183 and 1174 cm^{-1} are more intense as compared to the dark state spectrum. A strong band at 1183 cm^{-1} is characteristic for the 13-*cis* configuration of the retinal in *Np*SRII and BR [15,24]. Furthermore a downshift of about 3–5 cm^{-1} for the 1200 cm^{-1} band was already observed for the M state of *Hs*SRI and *Np*SRII [13,24]. Consequently, we conclude from the close accordance with M state spectra of sensory rhodopsins that in the P_2^{380} state 13-*cis* retinal is mostly present.

The RSB frequency shifts from 1646 cm^{-1} in the ground state (Fig. 3) to 1610 cm^{-1} in the P_2^{380} state (Fig. 4). Such a large downshift of 36 cm^{-1} was likewise detected for the formation of the 13-*cis* retinal in the M state of *Np*SRII (1652 to 1616 cm^{-1} [24]). Upon deuteration this band does not shift (Fig. 4, inset), implying that the C=N vibration is not influenced by hydrogen changes. This confirms clearly the presence of a deprotonated RSB in the conductive P_2^{380} state.

3.3. Light-induced FTIR difference spectroscopy on the P_2^{380} state

Whereas RR spectroscopy selects for the vibrations of the chromophore, the structural changes registered by FTIR difference spectroscopy also includes the protein moiety. Here, light-induced differences are recorded between the dark and the long-lived P_2^{380} state of *Ca*ChR1 (Fig. 5). The three negative bands at 1238 cm^{-1}, 1203 cm^{-1} and 1162 cm^{-1} can be assigned to C–C stretching vibrations of all-*trans* retinal [26], confirming that the photocycle starts predominantly from the all-*trans* form. The absence of positive bands in this frequency range indicates the predominance of a photocycle intermediate with deprotonated RSB [27,28]. This is in accordance with the result of the RR spectrum where the P_2^{380} intermediate with a deprotonated RSB predominantly accumulates under continuous illumination (Figs. 4 and S3). The small positive band at 1176 cm^{-1} corresponds to an intermediate accumulated to minor amounts together with the P_2^{380} state. This band most likely indicates the all-*trans* retinal from an O-like intermediate [29–31]. Overall, the changes in the retinal vibrations upon transition from the dark to the P_2^{380} intermediate as reflected by the FTIR difference spectrum are clearly assigned by comparison with the corresponding RR spectra (Fig. S3).

FTIR difference spectroscopy is also exquisitely suited to report on conformational changes of the protein backbone and on

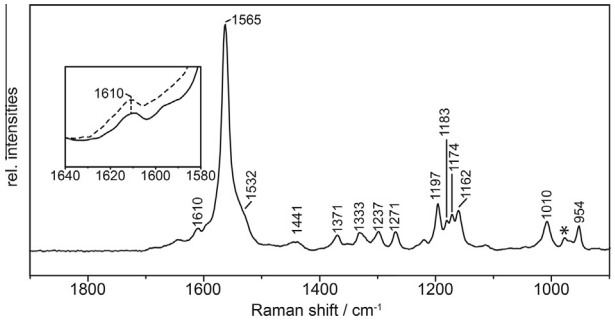

Fig. 4. Raman spectra of the P_2^{380} intermediate of *Ca*ChR1 obtained under photostationary conditions by illumination with 532 nm. Resonance Raman conditions are established with 413 nm. The inset shows a zoom out of the Raman spectra in H_2O (continuous line) and in D_2O (dashed line) in the 1640 and 1580 cm^{-1} region. The C=N stretching mode at 1610 cm^{-1} of the deprotonated RSB is invariant towards H/D exchange. The band labeled by an asterisk (*) is the same as in Fig. 3.

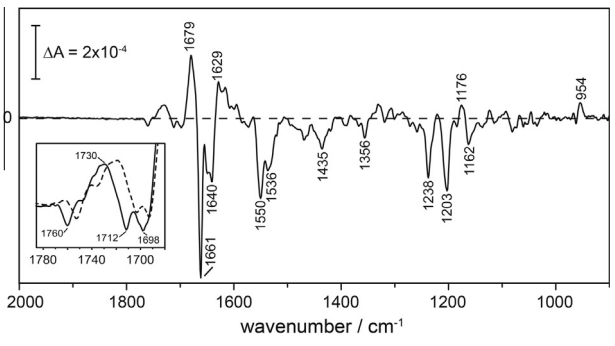

Fig. 5. Light-induced FTIR difference spectrum of *Ca*ChR1 recorded under continuous illumination with LED emitting at 505 nm. The carboxylic region between 1785 and 1680 cm^{-1} is shown as a zoom out (continuous line). All bands undergo a 5–10 cm^{-1} downshift in D_2O (dashed line).

protonation changes [32]. Strong difference bands appear in the amide I region (predominantly C=O stretch of the peptide bond in the 1620–1680 cm^{-1} region). The negative band at 1661 cm^{-1} was also observed in the open state (P_3^{520}) of *Cr*ChR2 [6,7] but the positive band at 1679 cm^{-1} is unique to *Ca*ChR1. Thus, we infer that the structural changes that lead to the opening of the two channelrhodopsins are slightly different. The C=O stretching vibration of protonated carboxylic groups appear in the 1780–1690 cm^{-1} frequency region [33,34]. Overall, the number of vibrational bands is significantly larger (Fig. 5, inset) as compared to FTIR difference spectra of any microbial rhodopsin, including *Cr*ChR2. Three negative bands at 1760 cm^{-1}, 1712 cm^{-1} and 1698 cm^{-1} and one large positive band feature centered at 1730 cm^{-1} are resolved in this region. The positive band is expected to correspond to the proton acceptor of the RSB, although its unusual width (full width at half maximum (FWHM) of 20 cm^{-1}) compared with typical values of 8 cm^{-1} for C=O stretching modes of carboxylic groups in proteins suggests the presence of several components. The three negative bands are likely due to aspartic or glutamic acid groups, that deprotonate or change their hydrogen bonding in the transition from the closed to the open state. The entire difference spectrum in this region exhibits a 5–10 cm^{-1} downshift in D_2O (see inset of Fig. 5). It will be of great interest to assign these vibrational bands to specific amino acid residues by mutational studies. In analogy to *Cr*ChR2, D299 and E169 are candidates as proton acceptors from the RSB [10], whereas D202 might be the proton donor (Fig. 1).

In summary, we determined the retinal isomer composition of dark state *Ca*ChR1 to an overall ratio of 70:30 all-*trans* to 13-*cis* retinal, which is in accordance to the retinal composition of *Cr*ChR2. Due to the high frequency of the protonated RSB vibration we infer the protonated RSB to be strongly hydrogen-bonded in the dark state. This hydrogen-bonding network might also contain a water molecule, as it was shown for BR [18,23]. For the first time, the Raman spectrum of the open (conductive) P_2 state of a channelrhodopsin was recorded and the frequency of the deprotonated RSB was determined. Hydrogen-bonding changes of carboxylic groups and amide I changes between the open and closed state were detected by FTIR difference spectroscopy. Compared to FTIR spectra of the conductive P_3^{520} state of *Cr*ChR2, the changes in amide I and carboxylic acid vibrations are different indicating distinctive structures for the conductive states in the two channelrhodopsins. This vibrational spectroscopic study opens an avenue to resolve the mechanism of *Ca*ChR1 and critically discuss differences and commonalities to *Cr*ChR2.

Acknowledgments

We thank D. Heinrich, K. Hoffmann, J. Wonneberg and I. Wallat for excellent technical assistance. This work was supported by the Leibniz Graduate School from the Leibniz Gesellschaft and by the Deutsche Forschungsgemeinschaft (SFB 1078/B3 to J.H. and B4 to R.S.).

Appendix A. Supplementary data

Supplementary data associated with this article can be found, in the online version, at http://dx.doi.org/10.1016/j.febslet.2014.05.019.

References

[1] Berthold, P., Tsunoda, S.P., Ernst, O.P., Mages, W., Gradmann, D. and Hegemann, P. (2008) Channelrhodopsin-1 initiates phototaxis and photophobic responses in *Chlamydomonas* by immediate light-induced depolarization. Plant Cell 20, 1665–1677.

[2] Prigge, M., Schneider, F., Tsunoda, S.P., Shilyansky, C., Wietek, J., Deisseroth, K. and Hegemann, P. (2012) Color-tuned channelrhodopsins for multiwavelength optogenetics. J. Biol. Chem. 287, 31804–31812.

[3] Hou, S.Y., Govorunova, E.G., Ntefidou, M., Lane, C.E., Spudich, E.N., Sineshchekov, O.A. and Spudich, J.L. (2012) Diversity of *Chlamydomonas* channelrhodopsins. Photochem. Photobiol. 88, 119–128.

[4] Lorenz-Fonfria, V.A. and Heberle, J. (2014) Channelrhodopsin unchained: structure and mechanism of a light-gated cation channel. Biochim. Biophys. Acta 10, 626–642.

[5] Kato, H.E. et al. (2012) Crystal structure of the channelrhodopsin light-gated cation channel. Nature 482, 369–374.

[6] Nack, M., Radu, I., Bamann, C., Bamberg, E. and Heberle, J. (2009) The retinal structure of channelrhodopsin-2 assessed by resonance Raman spectroscopy. FEBS Lett. 583, 3676–3680.

[7] Lorenz-Fonfria, V.A. et al. (2013) Transient protonation changes in channelrhodopsin-2 and their relevance to channel gating. PNAS 110, 1273–1281.

[8] Krause, N., Engelhard, C., Heberle, J., Schlesinger, R. and Bittl, R. (2013) Structural differences between the closed and open states of channelrhodopsin-2 as observed by EPR spectroscopy. FEBS Lett. 587, 3309–3313.

[9] Sattig, T., Rickert, C., Bamberg, E., Steinhoff, H.J. and Bamann, C. (2013) Light-induced movement of the transmembrane helix B in channelrhodopsin-2. Angew. Chem. Int. Ed. Engl. 52, 9705–9708.

[10] Sineshchekov, O.A., Govorunova, E.G., Wang, J., Li, H. and Spudich, J.L. (2013) Intramolecular proton transfer in channelrhodopsins. Biophys. J. 104, 807–817.

[11] Scharf, B., Hess, B. and Engelhard, M. (1992) Chromophore of sensory rhodopsin II from *Halobacterium halobium*. Biochemistry 31, 12486–12492.

[12] Scherrer, P., Mathew, M.K., Sperling, W. and Stoeckenius, W. (1989) Retinal isomer ratio in dark-adapted purple membrane and bacteriorhodopsin monomers. Biochemistry 28, 829–834.

[13] Haupts, U., Eisfeld, W., Stockburger, M. and Oesterhelt, D. (1994) Sensory rhodopsin I photocycle intermediate SRI380 contains 13-cis retinal bound via an unprotonated Schiff base. FEBS Lett. 356, 25–29.

[14] Imamoto, Y., Shichida, Y., Hirayama, J., Tomioka, H., Kamo, N. and Yoshizawa, T. (1992) Chromophore configuration of pharaonis phoborhodopsin and its isomerization on photon absorption. Biochemistry 31, 2523–2528.

[15] Smith, S.O., Pardoen, J.A., Lugtenburg, J. and Mathies, R.A. (1987) Vibrational analysis of a 13-cis-retinal chromophore in dark-adapted bacteriorhodopsin. J. Phys. Chem. 91, 804–819.

[16] Ritter, E., Piwowarski, P., Hegemann, P. and Bartl, F.J. (2013) Light-dark adaptation of channelrhodopsin C128T mutant. J. Biol. Chem. 15, 10451–10458.

[17] Berndt, A., Prigge, M., Gradmann, D. and Hegemann, P. (2010) Two open states with progressive proton selectivities in the branched channelrhodopsin-2 photocycle. Biophys. J. 98, 753–761.

[18] Hildebrandt, P. and Stockburger, M. (1984) Role of water in bacteriorhodopsin's chromophore: resonance Raman-study. Biochemistry 23, 5539–5548.

[19] Althaus, T., Eisfield, W., Lohrmann, R. and Stockburger, M. (1995) Application of Raman spectroscopy to retinal proteins Isr. J. Chem. 35, 227–251.

[20] Smith, S.O., Braiman, M.S., Myers, A.B., Pardoen, J.A., Courtin, J.M.L., Winkel, C., Lugtenburg, J. and Mathies, R.A. (1987) Vibrational analysis of the *all-trans*-retinal chromophore in light-adapted bacteriorhodopsin. J. Am. Chem. Soc. 109, 3108–3125.

[21] Mironova, O.S., Efremov, R.G., Person, B., Heberle, J., Budyak, I.L., Büldt, G. and Schlesinger, R. (2005) Functional characterization of sensory rhodopsin II from *Halobacterium salinarum* expressed in *Escherichia coli*. FEBS Lett. 579, 3147–3151.

[22] Radu, I., Bamann, C., Nack, M., Nagel, G., Bamberg, E. and Heberle, J. (2009) Conformational changes of channelrhodopsin-2. J. Am. Chem. Soc. 131, 7313–7319.

[23] Doukas, A.G., Pande, A., Suzuki, T., Callender, R.H., Honig, B. and Ottolenghi, M. (1981) On the mechanism of hydrogen-deuterium exchange in bacteriorhodopsin. Biophys. J. 33, 275–279.

[24] Tateishi, Y., Abe, T., Tamogami, J., Nakao, Y., Kikukawa, T., Kamo, N. and Unno, M. (2011) Spectroscopic evidence for the formation of an N intermediate during the photocycle of sensory rhodopsin II (phoborhodopsin) from *Natronobacterium pharaonis*. Biochemistry 50, 2135–2143.

[25] Ames, J.B., Fodor, S., Gebhard, R., Raap, J., Van den Berg, E., Lugtenburg, J. and Mathies, R.A. (1989) Bacteriorhodopsin's M412 intermediate contains 13-cis, 14-s-trans, 15-anti-retinal Schiff base chromophore. Biochemistry 28, 3681–3687.

[26] Smith, S.O., Lugtenburg, J. and Mathies, R.A. (1985) Determination of retinal chromophore structure in bacteriorhodopsin with resonance Raman spectroscopy. J. Membr. Biol. 85, 95–109.

[27] Gerwert, K. and Siebert, F. (1986) Evidence for light-induced 13-*cis*, 14-s-*cis* isomerization in bacteriorhodopsin obtained by FTIR difference spectroscopy using isotopically labelled retinals. EMBO J. 5, 805–811.

[28] Maeda, A. (1995) Application of FTIR spectroscopy to the structural study on the function of bacteriorhodopsin. Isr. J. Chem. 35, 387–400.

[29] Bousche, O., Sonar, S., Krebs, M.P., Khorana, H.G. and Rothschild, K.J. (1992) Time-resolved Fourier transform infrared spectroscopy of the bacteriorhodopsin mutant Tyr-185 → Phe: Asp-96 reprotonates during O

formation; Asp-85 and Asp-212 deprotonate during O decay. Photochem. Photobiol. 56, 1085–1095.
[30] Bergo, V.B., Ntefidou, M., Trivedi, V.D., Amsden, J.J., Kralj, J.M., Rothschild, K.J. and Spudich, J.L. (2006) Conformational changes in the photocycle of *Anabaena* sensory rhodopsin: absence of the Schiff base counterion protonation signal. J. Biol. Chem. 281, 15208–15214.
[31] Furutani, Y., Iwamoto, M., Shimono, K., Wada, A., Ito, M., Kamo, N. and Kandori, H. (2004) FTIR spectroscopy of the O photointermediate in pharaonis phoborhodopsin. Biochemistry 43, 5204–5212.
[32] Braiman, M.S., Mogi, T., Marti, T., Stern, L.J., Khorana, H.G. and Rothschild, K.J. (1988) Vibrational spectroscopy of bacteriorhodopsin mutants: light-driven proton transport involves protonation changes of aspartic acid residues 85, 96, and 212. Biochemistry 27, 8516–8520.
[33] Nie, B., Stutzman, J. and Xie, A. (2005) A vibrational spectral maker for probing the hydrogen-bonding status of protonated Asp and Glu residues. Biophys. J. 88, 2833–2847.
[34] Takei, K., Takahashi, R. and Noguchi, T. (2008) Correlation between the hydrogen-bond structures and the C=O stretching frequencies of carboxylic acids as studied by density functional theory calculations: theoretical basis for interpretation of infrared bands of carboxylic groups in proteins. J. Phys. Chem. B 112, 6725–6731.
[35] Kiefer, F., Arnold, K., Kunzli, M., Bordoli, L. and Schwede, T. (2009) The SWISS-MODEL repository and associated resources. Nucleic Acids Res. 37, D387–D392.
[36] Arnold, K., Bordoli, L., Kopp, J. and Schwede, T. (2006) The SWISS-MODEL workspace: a web-based environment for protein structure homology modelling. Bioinformatics 22, 195–201.
[37] Guex, N., Peitsch, M.C. and Schwede, T. (2009) Automated comparative protein structure modeling with SWISS-MODEL and Swiss-PdbViewer: a historical perspective. Electrophoresis 30 (Suppl. 1), S162–S173.